Version of Record: https://www.sciencedirect.com/science/article/pii/S037877881730484X
Manuscript_1886793f52c257d85e327a1e6fd68f77

# Multi-scale Urban System Modeling for Sustainable Planning and Design

**Tian Kuay LIM [a], Marcel IGNATIUS*[b], Martin MIGUEL[c], Nyuk Hien WONG[d], and Hann-Ming Henry JUANG[e]**

a.E-mail: lim_tian_kuay@ura.gov.sg
Urban Redevelopment Authority, 45 Maxwell Road, the URA Centre, Singapore 069118

b.E-mail: bdgmarc@nus.edu.sg
Department of Building, National University of Singapore, School of Design and Environment, 4 Architecture Drive, Singapore 117566.

c.E-mail: miguel.martin@u.nus.edu
Department of Building, National University of Singapore, School of Design and Environment, 4 Architecture Drive, Singapore 117566.

d.E-mail: bdgwnh@nus.edu.sg
Department of Building, National University of Singapore, School of Design and Environment, 4 Architecture Drive, Singapore 117566.

e.E-mail: henry.juang@noaa.gov
Environmental Modeling Center, DOC/NOAA/NWS/NCEP, Washington, D.C.

*Corresponding author*

## Abstract

The urban heat island (UHI) phenomenon has become a concern in many major cities worldwide, as high summer temperatures and poor wind flow can have negative impacts on city dwellers, particularly increasing energy demand for artificial cooling. This paper showcases how an Integrated Multi-scale Environmental Urban Model (IMEUM) can be employed to support planners, architects and engineers to assess the combined impacts of the UHI phenomenon and rising global temperatures due to climate change. IMEUM concept derives from downscaling environmental models from global scale (25km) to mesoscale (1km) and city scale (100m). Hence, this paper showcases a computationally efficient method which couples multi-scale atmospheric models with statistical model to estimate weather parameters. Developed under Singapore context, IMEUM can be utilized to incorporate appropriate UHI mitigation measures upfront in design process, consecutively bridging the gap between global and building scale. This paper also includes calibration of the IMEUM output using observations from ground sensors. Furthermore, by using case study of a hypothetical office building, this paper showcases how the IMEUM output can be fully converted into a localized weather data file for cooling load simulation. IMEUM is currently being developed further into integrated quantitative urban environment simulation tool (QUEST), which can be used to test the immediate microclimatic impact of development plans and assess their long term impacts under future climate change scenarios.

## Keywords

Urban climate modeling; urban heat island; spectral modeling; global climate modeling; weather prediction; weather data; ambient temperature; cooling load simulation; microclimate analysis; climate change.

## 1. Introduction

Urban heat island (UHI) is defined as the rise in temperature of any man-made area, resulting in distinctive 'warm island' in comparison to their non-urbanized or natural landscape surroundings. Several factors, such as diminishing of green area, low wind velocity due to poor urban ventilation, release of the anthropogenic heat, and change of street surface coating materials contribute to UHI, as shown in Figure 1 [1-6]. These may lead to overheating by human energy release and the absorption of solar radiation on low albedo surface and buildings.

This problem will be further aggravated by increasing demand on air conditioning, which will again lead to further increasing more greenhouse gas, and subsequently buildings energy usage [7-9]. Especially for the latter, there has been a substantial buildings energy usage intensification due to ambient temperature increase in cities. The energy consumption in the urban environment impacts the urban surface energy budget and leads to the emission of anthropogenic sensible heat and moisture into the atmosphere [10]. According to Santamouris [11], the average increase of the cooling demand of representative buildings is approximately 23%; it was based on data from 1970-2010 period. A study done by Sun and Augenbroe has shown that the UHI considerably modifies the urban climate and the ignorance of the UHI effect remarkably underestimates building total energy use in hot climate zones where cooling energy use is dominant [12].

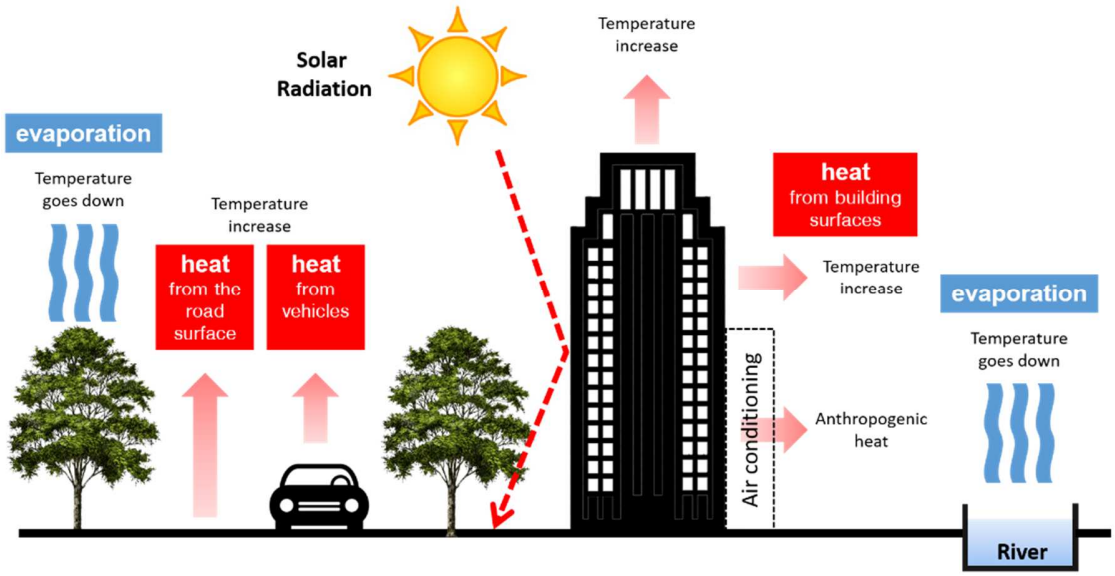


Figure 1. Schematic of urban heat island phenomena.

As a high-density city in the tropics, Singapore is similarly susceptible to high temperatures and the related negative impacts. Based on historical climate and developmental data spanning almost 50 years, the rapid urban expansion in Singapore is clearly reflected in spatially and temporally changing air and surface temperature patterns. The data have shown a doubling in the magnitude of the nocturnal canopy-layer UHI intensity between 1965 and 2004 and the expansion of the spatial extent of the nocturnal UHI with the development of new housing and industrial districts [13]. Changes in daily mean temperatures are projected to increase 1.4-4.6°C by end-century (2070-2099) with respect to the baseline period 1980-2009. From 1972 to 2014, annual average temperature has increased from 26.6°C to 27.7°C [14].

With a rapid pace of development in the coming years to meet population and economic needs, it is essential that the microclimatic impacts of these upcoming developments, as well as the long-term effects of climate change, are assessed early during the planning process. Moreover, appropriate design and mitigation measures are essential to be incorporated upfront in the plans.

The issue pertaining to UHI studies is the analysis segregation at different spatial scales; hence, it is crucial to link small-scale and mesoscale urban climate work, which has been deemed challenging due to complexity and non-linearity of urban climate system [15]. As highlighted by Mirzaei [16], there are three different scales in terms of UHI models diversification: building, micro, and city scale. Each scale model uses different approach with respect to the aim of study. However, each scale model has its own limitations and gaps which hinder a complete and comprehensive UHI investigation.

Multi-scale models are formed from integration of different types of models in order to cover the existing gap between them. Recently, to couple the microscale (building and/or urban canyon) and at the mesoscale (whole city), the building effect parameterization (BEP) and building energy model (BEM) was coupled with the U.S. Weather Research Forecasting (WRF) system. Within this coupling process, there are still various challenges such as initialization of the coupled model,, specification of a potentially vast number of parameters related to building characteristics (e.g. thermal properties, emissivity, albedo, anthropogenic heating, etc.), and model sensitivity to uncertainty in urban canopy parameters. Additionally, multiple nested domains as many as four were required to downscale the horizontal resolutions of the WRF domains from 24.3km to 0.9km [12, 17-19].

In relation to another crucial matter, it has also been mentioned how the UHI has aggravated the increase of energy demand due to achieving thermal comfort by means of heating or cooling with air conditioner. Hence, simulation packages for building performance analysis, particularly in energy and comfort, have become a paramount process in the building, or even master plan design. By default, these detailed building energy models assume that the weather conditions are uniformly distributed around the reference building. Consequently, the external heat gain of building envelope is not properly evaluated, and the effects of shading, greenery, anthropogenic heat or building surface materials on ambient temperature are often neglected. Hence, the relationship between the outdoor and indoor air quality is also often neglected.

Several studies have brought the issue of the available industry standard weather files for building simulation are not well suited to address the changing microclimate condition in cities due to city growth [12, 20-24]. These studies highlights the necessity of considering surrounding environment of a studied building in the process of looking at its energy performance; this can be done by integration of larger-scale models by incorporating urban morphology factors at precinct scale.

Hence, similar studies have also explored other ways to modify the existing weather climate data which have considered the changes in the climate, either for current study or future prediction [25-27]. Ignatius et al [28] showcases the significance of using the appropriate weather data by comparing urbanized temperature profile with the sensing data in Singapore context. It was found that there was a 1–2◦C disparity for average temperature, and the difference could reach

1.2–3.5◦C over peak afternoon period. Consequently, this temperature difference can lead to an approximately 8% difference in the predicted cooling load, 20% in external conduction gain, and 17% in fresh air intake gain; which was based on a controlled parametric study.

This contextual matter is deemed important to achieve adequate accuracy in conducting building energy analysis. The coupling method described above ensures that the building simulation analysis use the proper context, where the performance results reflect the surrounding microclimate and built environment.

Various studies suggest that continuing current patterns of development without intervention would produce degraded urban climates with further exacerbated urban temperatures [29-31]. With the enhanced greenhouse effect and global warming, the UHI is an extremely important issue to be addressed as the growing urban population could be further exposed to elevated temperatures. Current planning strategies for future urban development often target issues such as housing, transport, water and infrastructure; but few strategies comprehensively consider the urban climate and its interaction with the built environment [32]. With improved understanding of the interactions between the built environment and urban climates [9, 10, 15], many opportunities exist for those involved in urban planning and development to adopt this knowledge. Appropriate design and mitigation measures can then be incorporated upfront to minimize the risks of developing unfavorable urban climates [32-34].

This study seeks to develop a multi-scale urban system modeling for urban planners, architects, businesses stakeholders, and decision-makers to refine land use and development plans upfront. This is to minimize the risks of developing unfavorable urban climates, including climate change, in both the immediate and longer term future.

The multi-scale environmental urban model (IMEUM) is based on a multi-scale environmental urban models from global to a very high resolution mesoscale domain (as displayed in Figure 2) which is integrated with a multi-dimensional statistical model for weather variables estimation (wind, temperature and humidity) up to precinct level. This paper further addresses the necessity to link different temporal and spatial scales across multi-disciplinary approaches. The objective is to achieve better integration of measures, tools, and incorporation of urban morphology variables. This is to enhance existing and future development plans of the urban ecosystems; in which the whole process involve all players: urban planners, architects, businesses stakeholders, and government.

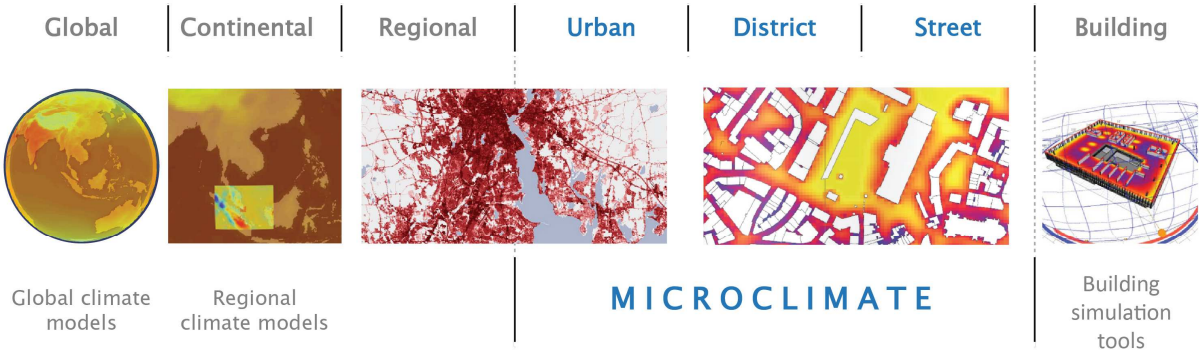


Figure 2. Urban climate modelling is based on multi-scale coupled environmental urban models from global up to street scale resolution (from macro to microclimate).

Hence, this paper showcases method which couples global-regional to mesoscale atmospheric models with multi-dimensional statistical model to estimate wind, temperature and humidity ranging from global scales to urban scales at the precinct level to support urban planning and design for the management of urban heat islands and global warming, thermal comfort, tree failures risk, and also for building energy analysis. This paper also includes calibration of the IMEUM output using mesoscale and local-scale observations from ground sensors.

To address the contextual matter on simulating building energy performance, this paper offers an alternative way on generating an urbanized microclimate weather data by utilizing the IMEUM, in which the outputs are subsequently converted into weather data to be used in a simulation package (EnergyPlus). The objective is to produce a more comprehensive energy performance simulation; in which under tropical climate, is highly defined by the cooling load performance due to air conditioning usage. A simple case study using a hypothetical office tower has been prepared to showcase the realization of the above mentioned models integration.

## 2. IMEUM development

### 2.1. Integrated multi-scale environmental urban model (IMEUM)

This methodology of scaling down global climate models (GCMs) outputs to be used at the local scale can be traced back to studies by Guan [35, 36], which adopted an effective procedure of considering the use of current weather condition, imposed offset, or diurnal modeling method to generate approximate future hourly weather data to study the impact of climate change on building. However, the Intergovernmental Panel on Climate Change (IPCC) acknowledged that GCMs outputs, typically having a horizontal resolution of between 250 and 600 km, were of too coarse for being directly used in regional climate change impact studies. Hence, regional climate models (RCMs), with higher resolution, have been developed for downscaling GCM simulations at the regional and local scales (see [37] and [38] for a review).

This section describes in brief the models used in the IMEUM, which elaborates the downscaling method (see Figure 3) from Global-Regional (25 km domain), to Mesoscale (1 km domain), and lastly City-urban scale (at site with the influence of urban morphology and greenery at 100 m domain). Overall, the IMEUM implements models across the different scales, namely: coupled Global-Regional Spectral model (GRSM) and Mesoscale Spectral model (MSM) and City-Urban model (CUM). For the latter, CUM adopts the Model Output Statistics (MOS) approach using

the Direct Model Output (DMO) values from the MSM (which is based on dynamical approach) as climate variables to be coupled with urban morphology variables (comprises urban morphology and greenery conditions at 100 m resolution). The following sub chapters describe how the IMEUM is developed for Singapore context, and its evaluation process by using on-site weather measurement for comparison.

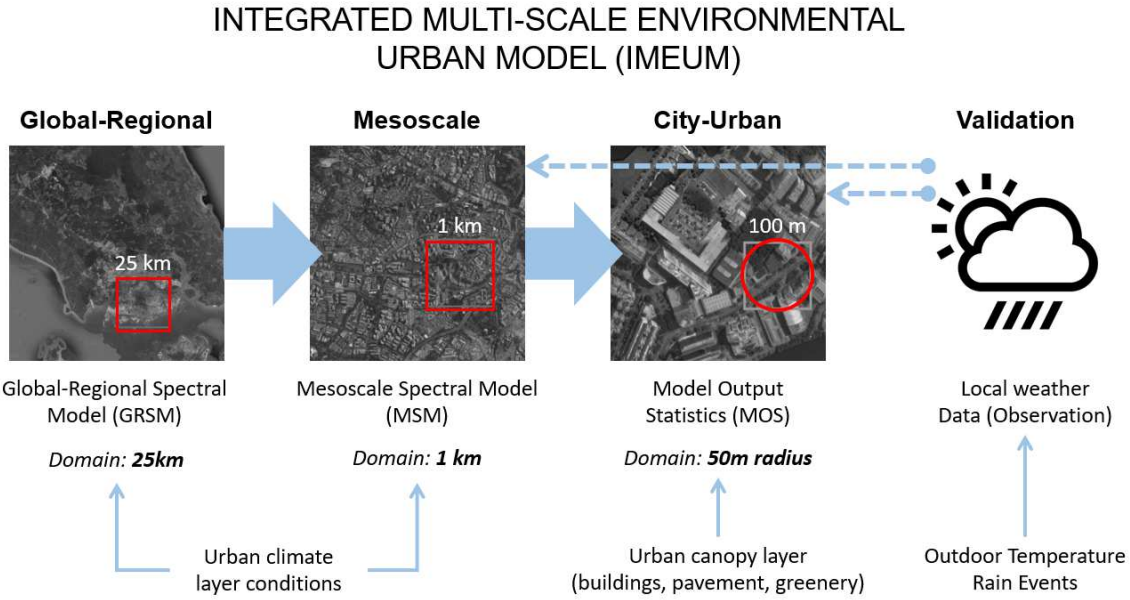


Figure 3. Overall methodology workflow of IMEUM, in which the final output is the microclimate estimation at city-urban scale. This has been calibrated using on-site observation data.

## 2.2. IMEUM scope: Singapore

Singapore, an island state located between 1º090′N to 1º290′N and 103º360′E to 104º250′E, has a typically wet equatorial climate [39] with uniformly high monthly mean temperature (26–27.7ºC) and annual rainfall (2,300 mm). At regional scale, Singapore experiences two seasons, namely, the Northeast Monsoon and Southwest Monsoon, which are interspersed with inter-monsoon conditions, squalls and local sea and land breezes.

For this study, the IMEUM is used for sustainable planning and design in addressing UHI and its impact on building cooling energy demand in Singapore. Essentially, UHI effect is evaluated based on the surface air temperature within urban areas and built-up areas relative to the surrounding rural areas. For the surface air temperature, it is related to the retention of solar heat in structures such as buildings, ground surfaces, and the emission and re-absorption of night time outgoing long-wave radiation by surrounding structures.

As this study will focus on clear weather conditions when the UHI effect will be the most pronounced, the IMEUM coupled GRSM-MSM has to be able to simulate fair or clear weather conditions to facilitate the study of UHI. In examining the hourly variation of the surface temperature (as shown in Figure 4), high surface air temperature is most frequent in Singapore from 9AM to 6PM throughout the year. It is also noted that the rain events, as displayed in Figure 5, are also the most frequent during the same period of the day throughout the year.

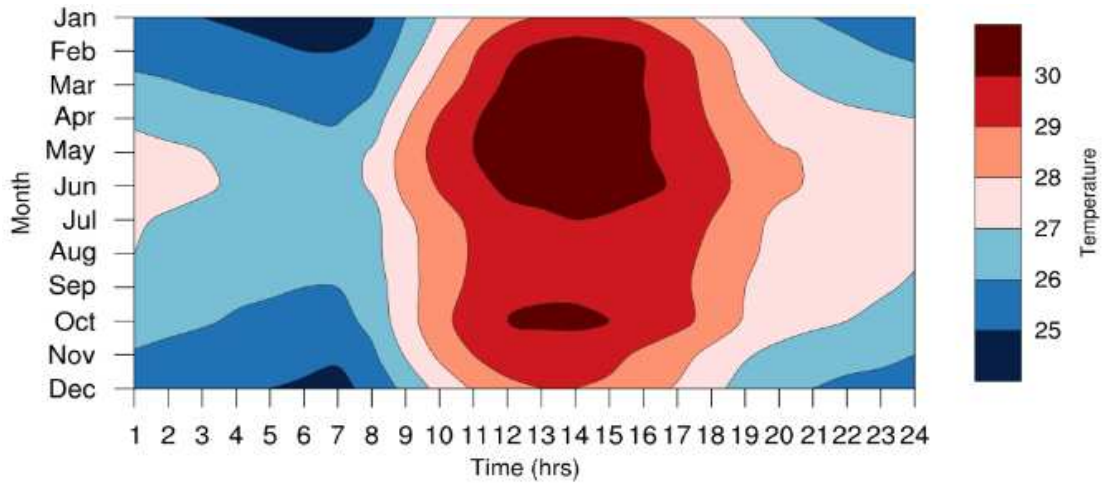


Figure 4. Hourly variation of temperature (ºC) for each month (1982-2015). Data from Changi Climate Station.

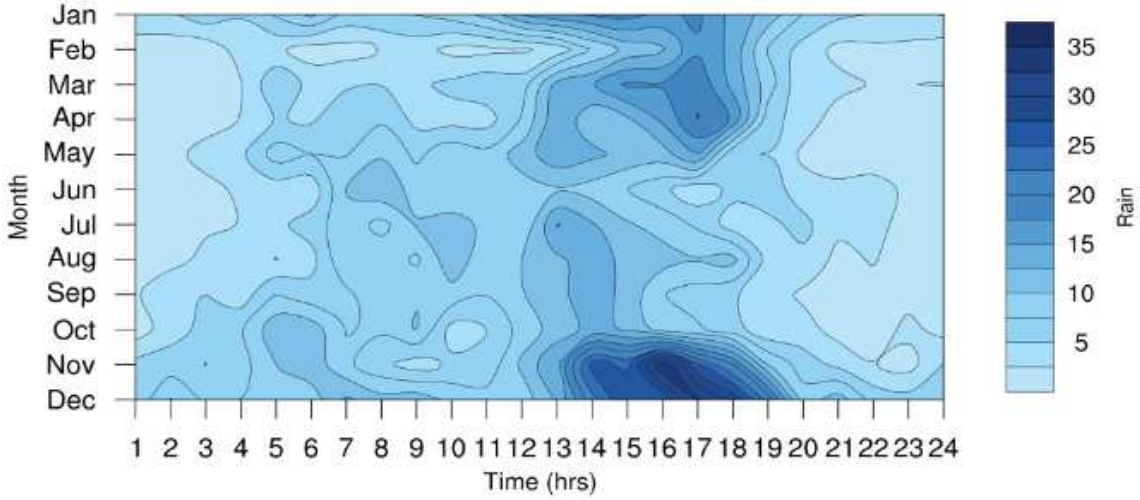


Figure 5. Hourly variation of rainfall (mm) for each month (1982-2015). Data from Changi Climate Station.

### 2.3. Coupled Global-Regional Spectral Model (GRSM) and Mesoscale Spectral Model (MSM)

Both GRSM and MSM are based on the operational National Centers for Environmental Prediction global spectral model (NCEP GSM) at T170L30/T384L64, NCEP regional spectral model (NCEP RSM) [40, 41] and NCEP mesoscale spectral model (NCEP MSM) [42]. The latter is the non-hydrostatic version of RSM that have been developed for high-resolution limited-area atmospheric model integration for weather forecast, seasonal prediction, and climate simulation [43-46] to support 10km 48-hr forecast over Hawaii islands, and 32km 63-hr forecast over Continental USA for short-range ensemble forecasts. These models have been adapted for Singapore with a spatial resolution of 1km. Using idealized experiments consisting of case studies of bubble convection and mountain waves at 10m spatial resolution [23], the NCEP MSM successfully produced acceptable simulations as compared to the analytical solutions. This implied that higher horizontal resolution of sub-1km of the MSM could be adapted for Singapore.

The primitive equations in sigma vertical coordinates are used for both GRSM and MSM. For these models, the uniqueness of the modelling approach is in its treatment of global-scale waves in global, regional, and mesoscale domains. While the large-scale motions, such as global wavenumbers 1-3, are well represented in the global spectral model, these global wave numbers cannot be handled properly in the regional or mesoscale spectral model. This is due to the limited spatial domain and may lead to an erroneous simulation of the global scale in the regional or mesoscale domain. With this modelling approach, the prognostic variable for MSM is separated into two parts: (1) *Based field*, which is based on large-scale model or analysis and well represented in the global spectral model, and (2) *Perturbation field*, which is computed by dynamic and physic models for the entire model domain.

The perturbation is integrated by spectral computation method. Due to the high accuracy of spectral method, this model is capable of fast spin-up and generating high accuracy mesoscale features. Also, due to the base field inclusion from large-scale model, the large-scale feature for the model results would not drift away. Thus, it is not only suitable for high-resolution weather forecast, but also excellent for long-term climate prediction, climate change impact, and for downscaling GCMs simulations down to regional and local scales. Significantly, the coupling of the GRSM and MSM uses a single nested domain to downscale the horizontal resolutions from 25km to 1km as. this is deemed to be more efficient as compared to the use of WRF [19] which required four nested domains for downscaling process from 24.3km to 0.9km. The perturbation equations for the MSM [42] are described in more detail in Appendix section.

In addition to the non-hydrostatic dynamics, the spectral models use a set of model physics: a package of short and longwave radiations (with diurnal variation and cloud interaction), a soil modeling physics, land surface physics which include an option for the NCEP – Oregon State University – U.S. Air Force–National Weather Service Office of Hydrologic Development (NOAH) land surface model (LSM) [47, 48], a high-resolution planetary boundary layer physics with a nonlocal vertical diffusion [49], gravity wave drag physics parameterization, shallow convection, cumulus convection parameterizations, and cloud physics which include cloud water, rain water, ice, snow, and graupel. Each of them can be turned on and off manually, especially convection parameterization and number of cloud constituents in cloud physics [50].

### 2.4. Evaluation of the IMEUM (coupled GRSM-MSM)

As previously mentioned, the horizontal resolution/grid sizes of the MSM domain is at 1.0km (256 x 128 resolution) for Singapore area, as shown in Figure 6. In the vertical direction, there are 42 sigma levels or vertical coordinates, defined by $\bar{p}/\bar{p}_s$, in which $\bar{p}$ refers to hydrostatic pressure and $\bar{p}_s$ refers to hydrostatic pressure at the surface. The time integration step was set at 10s. The initial conditions and lateral boundary conditions for the MSM were analyzed from the NCEP's 6-hourly operational Global Forecast System (GFS) at 25km resolution.

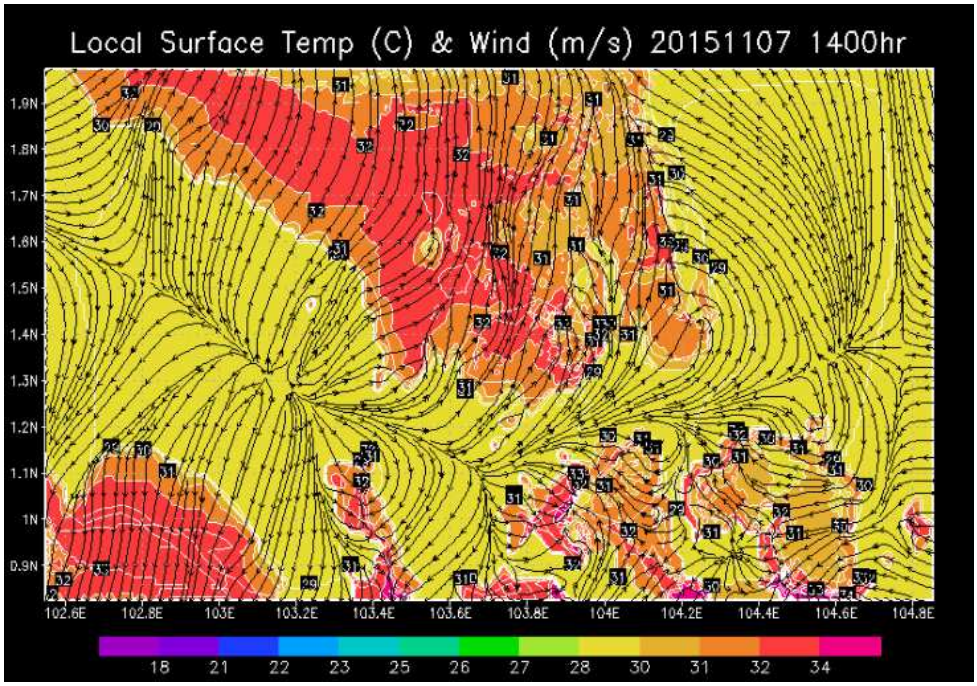


Figure 6. MSM domain (1.0km) for the study area.

High resolution observations of weather conditions for Singapore were available from Nov 2007 to Apr 2008 for the evaluation of the coupled GRSM-MSM (1.0km resolution) to simulate fair or clear weather conditions. These observations include the sensing data from weather radar (250m resolution) and in-situ rain gauges as shown in Figure 7 respectively.

The evaluation is based on skill scores recommendations for the verification and inter-comparison of Quantitative Precipitation Forecasts (QPFs) and Probabilistic Quantitative Precipitation forecasts (PQPFs) from operational NWP models, World Weather Research Programme (WWRP), World Meteorological Organization [51].

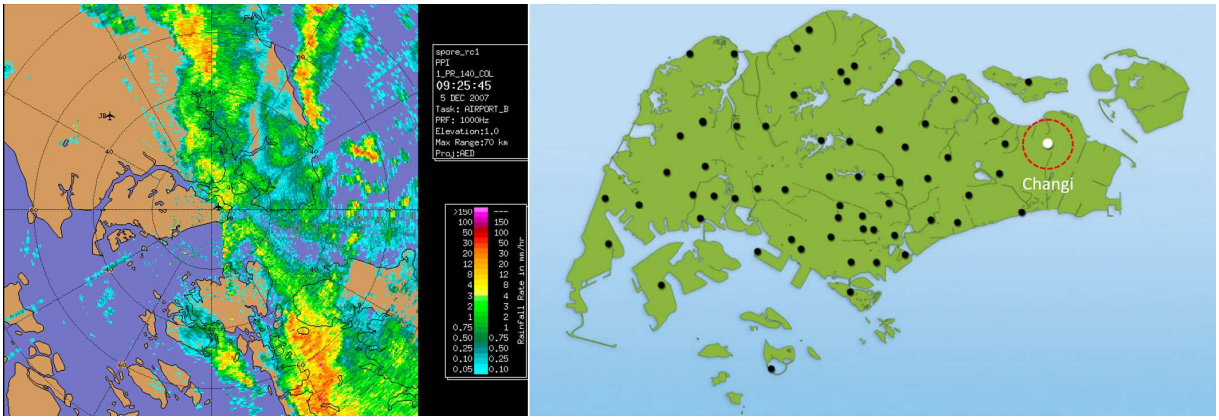


Figure 7. Sensing data from weather radar (left) and in-situ rain gauges (right) for the evaluation of the coupled GRSM-MSM. Data from Changi Climate Station.

To evaluate the GRSM-MSM capability in simulating fair weather and weather conditions with rain events, the highly recommended skill scores, namely: Proportion correct (PC) and Probability of detection (POD) were computed, as shown in the four-cell contingency table (Table 1 and Table 2) for 'Rain' and 'No Rain' events.

Table 1. Four cell contingency table, where a is the number of hits, b is the number of misses, c are the false alarms and d is the number of hits for forecasting no rain correctly.

| **Measured** | **Forecast** | |
|---|---|---|
| | Rain | No Rain |
| Rain | *a* | *b* |
| No rain | *c* | *d* |

Table 2. Parameters (based on the contingency Table1) applied to assess the quality of coupled Global-Regional Spectral Model-Mesoscale Spectral Model (GRSM-MSM) in simulating fair weather (no rain) and weather conditions (with rain).

| Description | Formula | Range | Perfect | Meaning |
|---|---|---|---|---|
| Percentage correct (PC) | $PC = \frac{a+d}{a+b+c+d} x100\%$ | [0,100] | 100% | Insensitive to rarer precipitation events. |
| Probability of detection (POD), Hit Rate (HR) [52] | $POD = \frac{a}{a+b}$ | [0,1] | 1 | Proportion of rain events, which were correctly predicted. |

*

Table 3. PC and POD skill scores over the study area.

| | **9hr** | **10hr** | **11hr** | **12hr** | **13hr** | **14hr** | **15hr** | **16hr** | **17hr** | **18hr** |
|---|---|---|---|---|---|---|---|---|---|---|
| PC (%) | 89 | 87 | 84 | 82 | 86 | 84 | 77 | 79 | 84 | 80 |
| POD | 0.90 | 0.89 | 0.96 | 0.96 | 0.97 | 0.93 | 0.85 | 0.87 | 0.86 | 0.73 |

The skill scores for PC and POD over the study area are shown in the Table 3. These skill scores showed that the IMEUM coupled GRSM-MSM is able to simulate fair or clear weather conditions. The DMO values such as surface temperature, wind, and mean sea-level pressure from the coupled GRSM-MSM were used for the City-Urban Model (CUM) component as climate predictors to simulate the ambient temperature condition, added with the influence of surrounding buildings, pavement, and proposed greenery options.

## 2.5. City-Urban Model (CUM), a Dynamical-Statistical Approach

For the development of the IMEUM MSM, there are deficiencies in some of the physics parameterization in the atmospheric model. For instance, a key source of model deficiencies in the simulation of precipitation is caused by the convective parameterization. To address these deficiencies, statistical downscaling approaches, which make use of the simulated high resolution atmospheric conditions, are incorporated for the IMEUM development for the city scale. The rationale is to establish statistical relationships between variables (predictors) simulated by the atmospheric model and local-scale observations (predictands) to correct model errors.

One of the most established techniques for accomplishing this is called Model Output Statistics (MOS). This technique, together with screening regression, has been applied to the prediction of surface wind, probability of precipitation, maximum temperature and cloud amount [53, 54]. For the IMEUM City-Urban Model (CUM), the MOS technique is adopted and it uses the DMO values from the MSM as climate predictors coupled with urban morphology predictors. The latter component comprises buildings, pavement, and greenery conditions going up to 100m resolution.

The MOS technique refers to the already established empirical prediction models which uses multiple variables to calculate the minimum, average and maximum air temperature ($T_{min}$, $T_{avg}$, and $T_{max}$) for a point of interest. As shown in Figure 8, the predictors comprises: (1) *climate predictors* ($RefT_{min}$, $RefT_{avg}$, and $RefT_{max}$); and (2) *urban morphology predictors* (surrounding buildings consideration, surface customization, and proposed greenery options), based on a 50-m radius urban built up area in Singapore [55-59].


**Climate Predictors**

Ref $T_{min}$ (°C) = daily minimum ambient temperature
Ref $T_{avg}$ (°C) = daily average ambient temperature
Ref $T_{max}$ (°C) = daily maximum ambient temperature

Pre-calculated by IMEUM GRSM-MSM

**Urban Morphology Predictors**

PAVE (%) = % of pavement area over R50m area
BDG (%) = % of building footprint over R50m area
HBDG = average building height/BDG ratio over R50m area
WALL ($m^2$) = total wall surface area
GnPR = Green plot ratio
SVF = Sky view factor
ALB = average surface albedo

Figure 8. Independent variables used in IMEUM City-urban model (CUM).

The air temperature prediction models can be written as follows:

$T_{max}$ (°C) = 4.494+ 0.695 Ref $T_{max}$ (°C) + 0.001 SOLARmax ($W/m^2$) - 0.39WINDmax + 0.008 PAVE(%) – 0.002 Avg Height (m) + 1.078SVF + 32.235 ALB (1)

$T_{avg}$ (°C) = 2.676 + 0.919 Ref $T_{avg}$ (°C) – 0.201 GnPR – 0.015 HBDG + 1.520E-05 WALL ($m^2$) + 0.240 SVF (2)

$T_{min}$ (°C) = 2.116 + 0.932 Ref $T_{min}$ (°C) – 0.272 GnPR + 0.003 PAVE - 0.004 HBDG + 1. 619 E-05 WALL ($m^2$)– 1.33 ALB (3)

In order to simulate the ambient temperature conditions ($T_{min}$, $T_{avg}$, and $T_{max}$) at a certain area, the models require reference weather data, which are usually obtained from weather stations. In this case, those reference data ($Ref\ T_{min}$, $RefT_{avg}$ and $Ref\ T_{max}$) have been pre-calculated by IMEUM GRSM-MSM.

To develop the output into a functional weather data (e.g. to be used for EnergyPlus simulation), it needs to be converted into hourly diurnal ambient temperature data. An empirical model was utilized to generate 24-h temperature profile for a typical day, using both reference and predicted

values. This method has been used in the previous study to showcase the importance of generating local temperature condition on conducting building energy performance [28].

If $X_t < X_{avg}$,

$$T_t = T_{min} + (X_t - X_{min}) \frac{(X_{max} - X_{min})}{(X_{avg} - X_{min})^2} \frac{(T_{avg} - T_{min})^2}{(T_{max} - T_{min})} \quad (4)$$

If $X_t > X_{avg}$,

$$T_t = T_{max} - (X_{max} - X_t) \frac{(X_{max} - X_{min})}{(X_{max} - X_{avg})^2} \frac{(T_{max} - T_{avg})^2}{(T_{max} - T_{min})} \quad (5)$$

where $X_t$ is the outdoor air temperature pre-calculated by the IMEUM GRSM-MSM at day $d$ at hour $t$ (from 00:00 to 23:00). Subsequently, the temperatures $X_{min}$, $X_{avg}$ and $X_{max}$ represents the climate predictors ($RefT_{min}$, $RefT_{avg}$, and $RefT_{max}$).

### 2.6. Evaluation of the IMEUM City-Urban Model (CUM)

These prediction models, which were adopted for the MOS technique, were based on the empirical data collected over a period of close to 3 years as part of the development of an assessment method to evaluate the impact of estate development, which includes the assessment method of existing greenery condition and proposed master plan in an estate development. Overall, weather sensors and loggers were installed at 10 different areas representing land uses such as business parks, industrial estates, business districts, parks, and housing estates. Location details can be observed in both Figure 9 and Table 4. Moreover, the empirical models have been validated in the previous study by comparing field measurement results with the predicted results. It was concluded that there is a good agreement between predicted and measured data [60].

It is important to note also that the field measurement data used were influenced by anthropogenic heat and moisture from buildings and traffic up to a certain degree and as well as moisture from greenery via evapotranspiration [61]. However, it was unable to be isolated as an independent variable and furthermore it is not the main focus of the study.

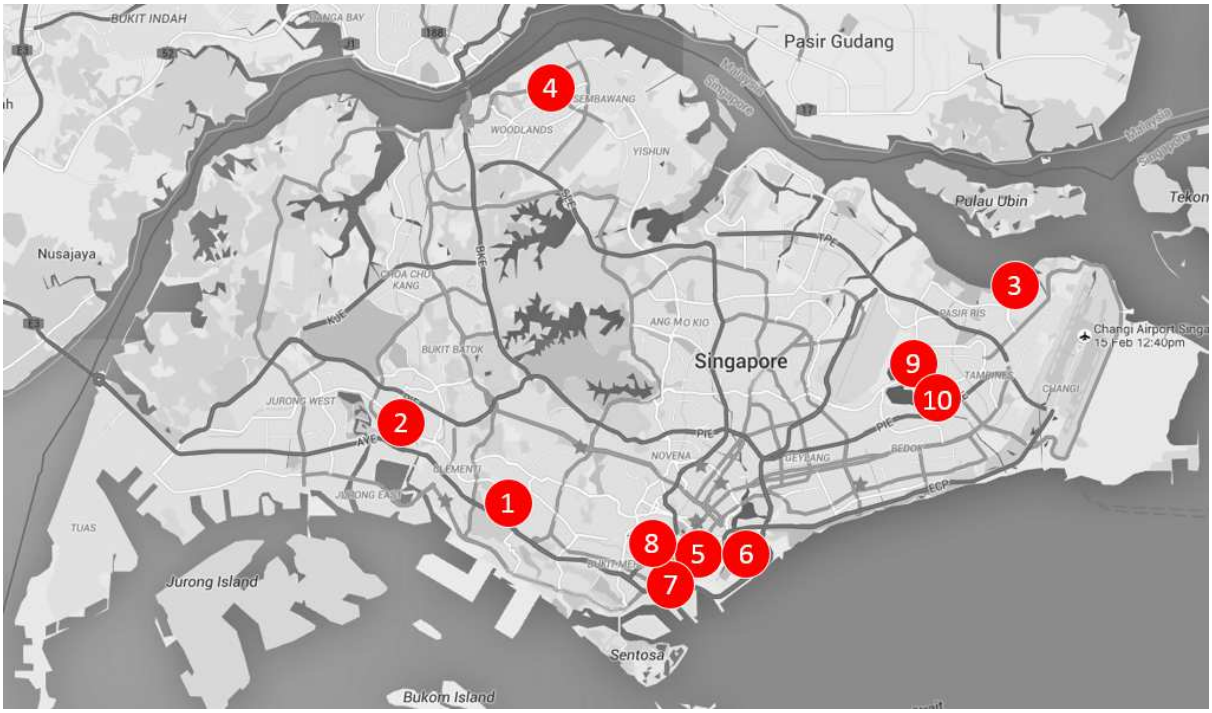

Figure 9. Field measurement conducted in various locations to support the MOS development.

Table 4. Field measurement locations and number of measurement points for each area.

| No | Area | Number of measurement points |
|---|---|---|
| 1 | One-North Business Park | 30 |
| 2 | International Business Park | 10 |
| 3 | Loyang Industrial Estate | 11 |
| 4 | Woodlands Industrial Park | 12 |
| 5 | Marina Bay Promenade and Promontory | 8 |
| 6 | Gardens by the Bay | 4 |
| 7 | Shenton Way | 7 |
| 8 | Tanjong Pagar | 7 |
| 9 | Tampines | 4 |
| 10 | Bedok | 12 |
| | **Total** | **105** |

## 3. IMEUM application using case study

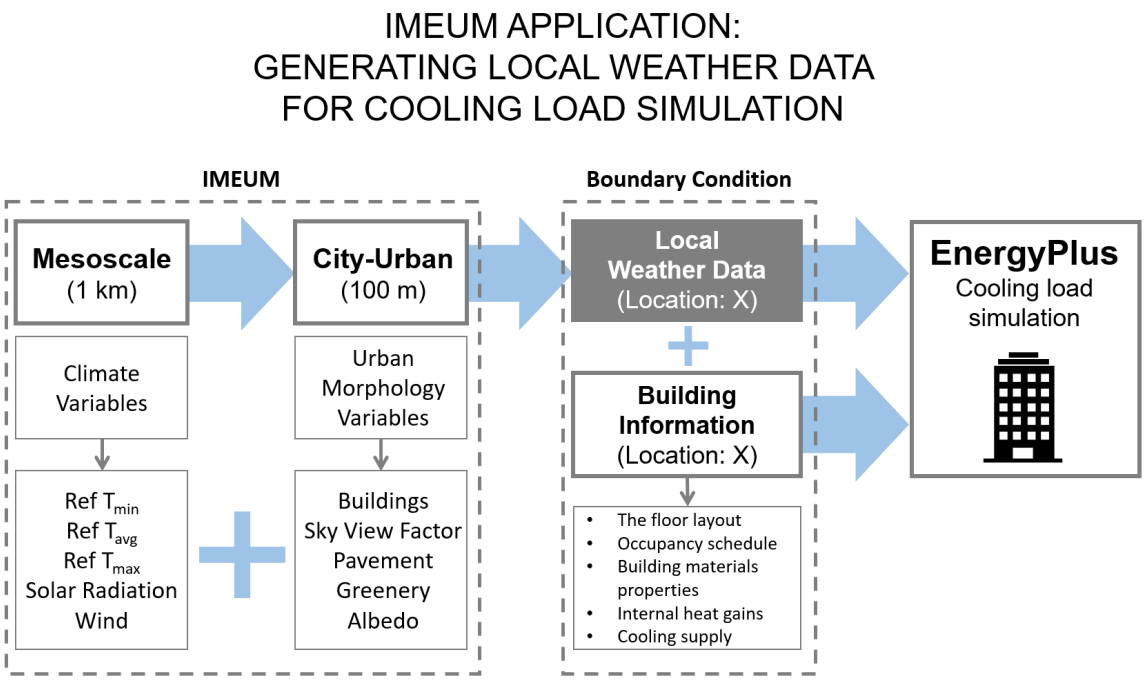


Figure 10. Workflow on using IMEUM to generate a local weather data for cooling load simulation.

This section showcases how to use the IMEUM output to be implemented in a building simulation software, especially for cooling load simulation. The workflow of this process can be seen in Figure 10. A hypothetical office building has been prepared on a real site located in West Singapore. Moreover, in situ sensing data from multiple measurement points located nearby the site were used in the process of evaluating the IMEUM output. The weather sensors were spread over an area of 1.0km radius, as shown in Figure 11. Point A, B, and C were chosen as reference points to be compared with the IMEUM output in terms of evaluating the accuracy of the climate modeling up to precinct level.

A 20-storey hypothetical office building has been placed nearby station A for building simulation using EnergyPlus, which is known as building energy models, capable of simulating the energy performance based on outdoor-indoor energy balance. However, since the influence of neighboring buildings are neglected in EnergyPlus, there is a lack of integration with larger scale models, especially if one would like to investigate the UHI effect on buildings. Hence, this is where the role of IMEUM becomes significant: to provide the corrected weather data due to the surroundings urban morphology conditions.

Thus, as displayed in Figure 10, this chapter showcases the integration of IMEUM, a combination of city-scale and micro-scale models, with EnergyPlus as building energy model. Together, the cooling load simulation has already considered the impact of surrounding microclimate condition which is affected by urban morphology and greenery presence. The objective is to illustrate how the model output from IMEUM, which has been transformed into hourly data, can be used as localized weather data in EnergyPlus to conduct the simulation. The

simulation period was established for 4 days from 7 to 10 January 2016, as those have been considered as fairly calm days. The floor layout, occupancy schedule, building materials properties, internal heat gains, and cooling supply of the EnergyPlus model were defined as in Martin et al. [62]. The structure of the building developed with EnergyPlus is shown in Figure 12.

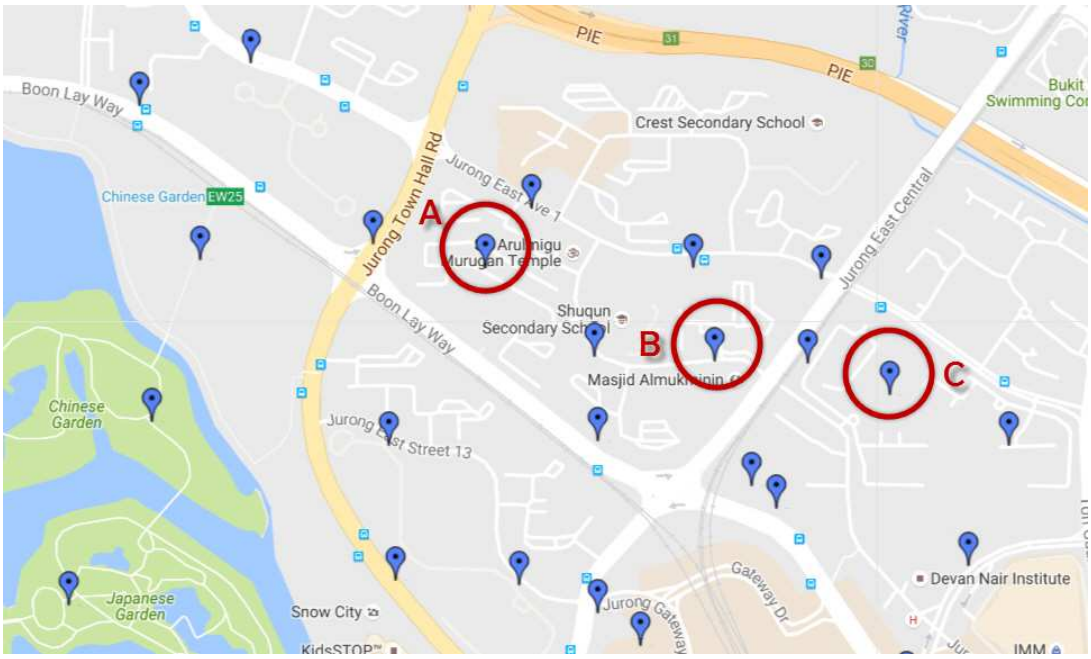


Figure 11. On-site weather measurement points, where point A, B, and C were selected to be used for case study evaluation.

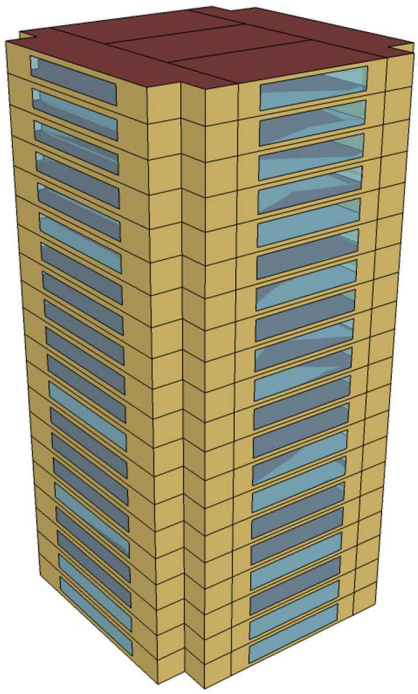

Figure 12. 20-storey building used to test outputs provided by IMEUM for building energy assessment.

## 4. Results and discussion

### 4.1. IMEUM output: localized weather data

The capability of the IMEUM in simulating the local hourly temperatures at 100m resolution was evaluated using the in-situ sensing data, for temperatures for the period from 7 to 10 January 2016. The temporal variation of the local hourly temperatures at 100m resolution compared reasonably well with the observed in-situ temperatures at Station A, B, and C (see Figure 13). One can observe that the method described in this paper was able to follow the upward, peak, downward trend of the sensing data. Hence, it is capable to simulate the ambient temperature by considering various weather components and the impact of built environment with adequate degree of confidence.

The simulated values of the local hourly temperatures at 100m resolution from the IMEUM were used as boundary conditions for the EnergyPlus Model to compute the cooling load energy consumption of a hypothetical office building at the location near Station A.

Essential weather variables for 4 days period were compiled to be converted into an EnergyPlus weather data file (.epw format), where variables such as (1) outdoor temperature, (2) wind speed, and (3) mean sea level pressure were obtained from the IMEUM output. To complete the data set, data such as relative humidity (RH) and solar radiation are also required, in which were obtained from the Department of Geography weather station at National University of Singapore [63], the nearest data available from the study location. The time series charts of the 4 days weather data can be seen in Figure 14.

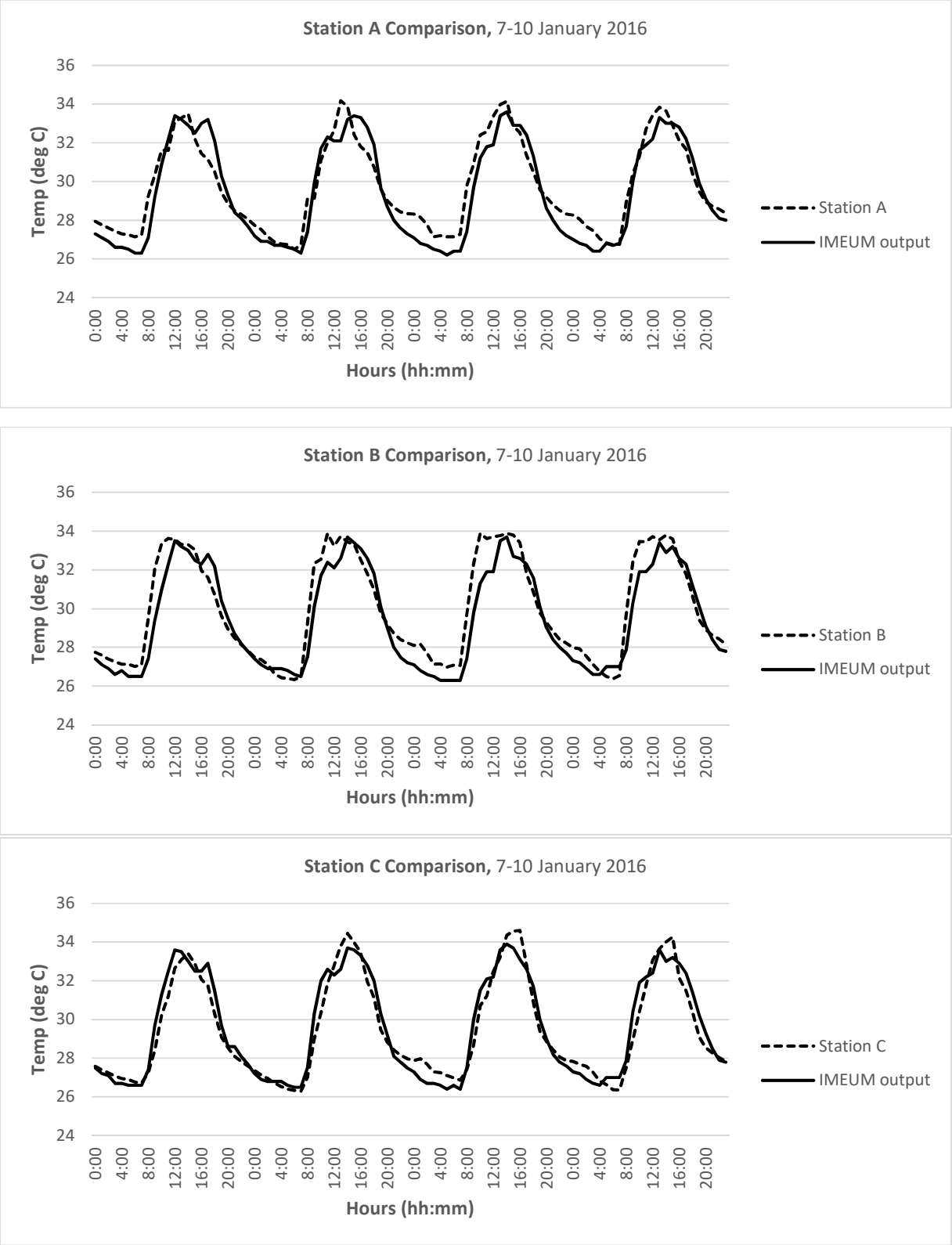


Figure 13. Ambient temperature comparison between sensing data and calculated method from IMEUM across three different locations.

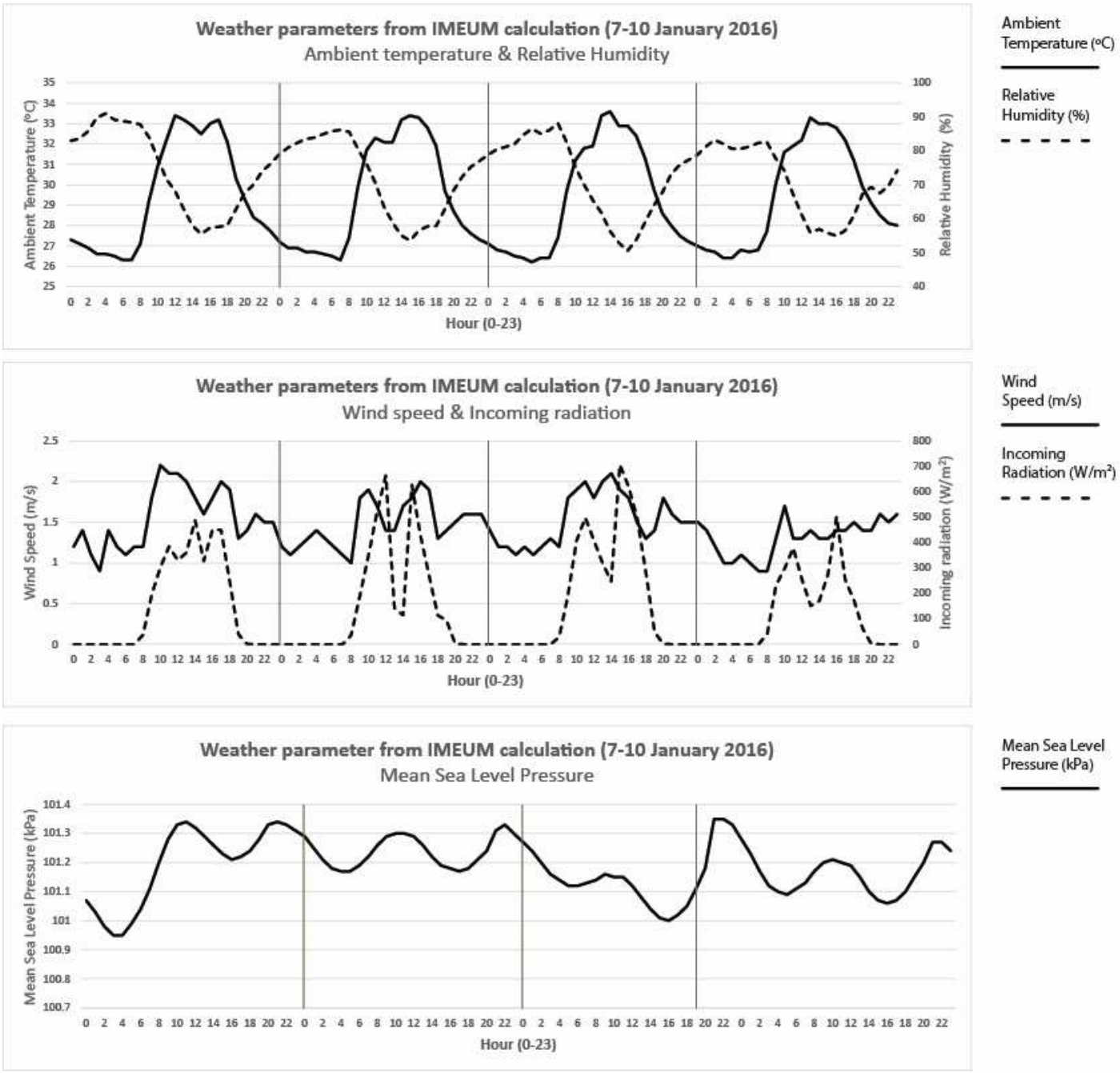


Figure 14. IMEUM final output comprises weather parameters at local scale.

### 4.2. Energy simulation with EnergyPlus

Figure 15 illustrates the ideal cooling load estimated from the EnergyPlus model of a 20-storey office building in Singapore. As mentioned earlier, weather conditions assessed from IMEUM were used as input of the model. By ideal cooling load, it is meant the exact amount of heat (per unit of time) that must be removed from the indoor air volume to keep both temperature and humidity at a given range. In this case, it was also assumed the HVAC system has infinite capacity. This outcome demonstrates that the cooling energy use is the highest the first two days (i.e. Thursday and Friday), lower the next day (i.e. Saturday), and the lowest the last day (i.e. Sunday). In this study, the last day is the most interesting case. To determine whether weather conditions assessed from IMEUM have an impact on the cooling load estimated by EnergyPlus, the internal heat gain was set to zero while cooling is assumed to be still supplied. On Sunday, it can be observed that the cooling load achieves its peak value during the middle of the day. Consequently, the cooling load seems to follow the diurnal temperature profile on Sunday.

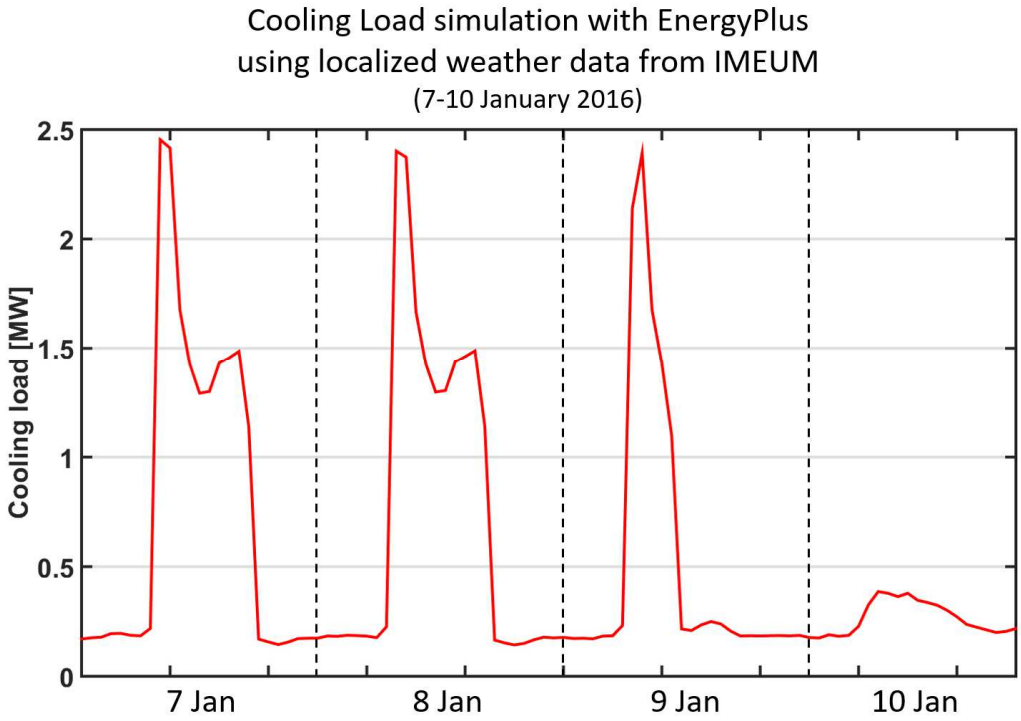


Figure 15. Ideal cooling load as estimated by the EnergyPlus model using weather conditions assessed from IMEUM.

## 5. Conclusions

### 5.1. Multi-layer climate modeling for urban planning

This paper showcased an alternative method on generating an urbanized microclimate weather data, which has been downscaled from the global scale. The method have considered multi variables ranging from climatic parameters (such as temperature and wind) to urban morphology factors (such as buildings, pavement, and vegetation). Comparison analysis of the model output with the in situ sensing data has shown a good agreement, in which the model is able to create

the similar temperature profile of a specific urban area within 50m radius of influence. Furthermore, the later chapter illustrates how the outcome of IMEUM was consolidated into a typical weather data to be used in EnergyPlus. The results showed that cooling load performance of a building can be properly simulated by using the urbanized weather data.

With the motivation for sustainable development and to better adapt to climate change, this study showcases the development of IMEUM with its capability to incorporate multi-scale modeling from global to local scale in an urban environment. Furthermore, the case study presented here showcases how the method is able to assess the impact of the UHI phenomenon on cooling energy consumption of a typical building.

The novelty of IMEUM method is its computationally efficient approach via coupled GRSM-MSM with MOS-EnergyPlus as compared to other computationally intensive approaches (e.g. the coupled WRF with energy models). This is mainly because this coupling technique implements dynamic statistical approach and an efficient dynamical nesting approach on scaling down the climate model into the local scale. Furthermore, it also considers the surrounding urban morphology factors at the local/precinct scale. Hence, the IMEUM method facilitates easy simulations to optimize the adoption of UHI and climate change mitigation strategies to support urban planning and design. Planners, architects and engineers can utilize this method to evaluate upfront appropriate mitigation measures and strategies involving parameters such as greenery, building heights, footprint and wall, albedo, etc., in urban planning and design process.

### 5.2. Future Works

Singapore will be undergoing a rapid pace of development in the coming 5-15 years, as new housing estates and growth areas are planned for development to meet population and economic needs by 2030. As the built environment contributes to the generation and trapping of heat, it is essential that the microclimatic impacts of these upcoming developments, as well as the long term effects of climate change, are assessed early during the planning process, and for the appropriate design and mitigation measures to be incorporated upfront in the plans. Hence, the objective of this study is to leverage on existing efforts and initiatives to develop an operational and integrated quantitative urban environment simulation tool or QUEST, which is lacking now.

IMEUM is currently being developed to support QUEST to function as an automated and seamless simulation tool that is operation-ready for end-users such as planners, architects, engineers in relevant agencies and potentially even the industry, to refine upcoming land use and development plans for maintaining good thermal comfort in both the immediate and longer term future. It would provide the end-users with a graphical user interface for them to specify the targeted locality/region and the past/current/future climate conditions to generate a set of baselines and future scenarios based on urban planning methodology, geospatial data on land-use, urban redevelopment of buildings, etc. Based on these specifications, QUEST, as a simulation tool, would automatically and seamlessly trigger a set of simulation workflow to generate the various parameters, namely: temperatures, wind and thermal comfort index for the targeted locality/region, and not limited to energy study, which has been showcased in this paper.

## 6. Acknowledgement

The authors wish to thank members of the staff at the Singapore Land Authority, the National Environment Agency (NEA) and the Urban Redevelopment Authority (URA) for the support of this work. Lim Tian Kuay wish to thank Mr Ronnie Tay (NEA), Mr Richard Hoo (URA), Prof Raj Thampuran (A*STAR) and Dr Vijay Tallapragada at NOAA's NCEP/EMC for their support and encouragement.

## 7. Abbreviations

| | | |
|---|---|---|
| BEM | = | Building energy model |
| BEP | = | Building effect parameterization |
| CUM | = | City-urban model |
| DMO | = | Direct model output |
| GCM | = | Global climate models |
| GSM | = | Global spectral model |
| GRSM | = | Global-regional spectral model |
| ICT | = | Information and communications technologies |
| IMEUM | = | Integrated multi-scale environmental urban model |
| IPCC | = | Intergovernmental Panel on Climate Change |
| LSM | = | Land surface model |
| MOS | = | Model output statistics |
| MSM | = | Mesoscale spectral model |
| NCEP | = | National Centers for Environmental Prediction |
| PC | = | Proportion correct |
| POD | = | Probability of detection |
| PQPF | = | Probabilistic Quantitative precipitation forecasts |
| QPF | = | Quantitative precipitation forecast |
| QUEST | = | Quantitative urban environment simulation tool |
| RCM | = | Regional climate model |
| RSM | = | Regional spectral model |
| UHI | = | Urban heat island |
| WMO | = | World Meteorological Organization |
| WRF | = | Weather Research Forecasting |
| WWRP | = | World Weather Research Programme |

## 8. References

1. Takahashi, K., et al., *Measurement of thermal environment in Kyoto City and its prediction by CFD simulation.* Energy and Buildings, 2004. **16**: p. 771–779.
2. Oke, T.R., *Boundary Layer Climates*. 1987, London: Routledge.
3. Oke, T.R., *City size and the urban heat island.* Atmospheric Environment, 1973. **7**: p. 769-779.
4. Chen, Y. and N.H. Wong, *Thermal benefits of city parks.* Energy and Buildings, 2006. **38**: p. 105-120.
5. Chong, Z.M.A., et al., *The Effect of Urban Heat Island on Heat Gain Increase*, in *The 8th International Conference on Urban Climates (ICUC8)*. 2012: Dublin, Ireland.

6. Jusuf, S.K. and N.H. Wong, *Valuing Green Spaces as a Heat Mitigation Technique*, in *Urban Climate Mitigation Techniques*, M. Santamouris and D. Kolokotsa, Editors. 2016, Routledge: London. p. 41-62.
7. Crutzen, P.J., *The growing urban heat and pollution ''island'' effect—impact on chemistry and climate.* Atmospheric Environment, 2004. **38**: p. 3539–3540.
8. Santamouris, M., et al., *Energy and Climate in the Urban Built Environment*, ed. M. Santamouris. 2001, London, UK: James & James.
9. Santamouris, M., et al., *On the impact of urban heat island and global warming on the powerdemand and electricity consumption of buildings—A review.* Energy and Buildings, 2015. **98**.
10. Sailor, D.J., *A review of methods for estimating anthropogenic heat and moisture emissions in the urban environment.* International Journal of Climatology, 2011. **31**: p. 189-199.
11. Santamouris, M., *On the energy impact of urban heat island and global warming on buildings.* Energy and Buildings, 2014. **82**: p. 100–113.
12. Sun, Y. and G. Augenbroe, *Urban heat island effect on energy application studies of office buildings.* Energy and Buildings, 2014. **77**: p. 171-179.
13. Roth, M. and W.T.L. Chow, *A historical review and assessment of urban heat island research in Singapore.* Singapore Journal of Tropical Geography, 2012. **33**: p. 381–397.
14. MEWR. *Using Energy Responsibly: Climate Change*. 2016 [cited 2016; Available from: http://www.mewr.gov.sg/topic/climate-change.
15. Arnfield, A., *Two decades of urban climate research: a review of turbulence, exchanges of energy and water, and the Urban Heat Island.* International Journal of Climatology, 2003. **23**: p. 1-26.
16. Mirzaei, P.A., *Recent challenges in modeling of urban heat island.* Sustainable Cities and Society, 2015. **19**: p. 200-206.
17. Chen, F., et al., *The integrated WRF/urban modelling system: development, evaluation,and applications to urban environmental problems.* International Journal of Climatology, 2011. **31**: p. 273–288.
18. Chow, W.T.L., et al., *A multi-method and multi-scale approach for estimating city-wide anthropogenic heat fluxes.* Atmospheric Environment, 2014. **99**: p. 64-76.
19. Li, X.-X., et al., *A multi-resolution ensemble study of a tropical urban environment and its interactions with the background regional atmosphere.* Journal of Geophysical Research: Atmospheres, 2013. **118**: p. 9804–9818.
20. Jentsch, M.F., A.S. Bahaj, and P.A.B. James, *Climate change future proofing of buildings—Generation and assessment of building simulation weather files.* Energy and Buildings, 2008. **40**: p. 2148–2168.
21. Jentsch, M.F., et al., *Transforming existing weather data for worldwide locations to enable energy and building performance simulation under future climates.* Renewable Energy, 2013. **55**: p. 514-524.
22. Chan, A.L.S., *Developing a modified typical meteorological year weather file for Hong Kong taking into account the urban heat island effect.* Building and Environment, 2011. **46**: p. 2434-2441.
23. Chan, A.L.S., *Developing future hourly weather files for studying the impact of climate change on building energy performance in Hong Kong.* Energy and Buildings, 2011. **43**: p. 2860–2868.
24. Kolokotroni, M., I. Giannitsaris, and R. Watkins, *The effect of the London urban heat island on building summer cooling demand and night ventilation strategies.* Solar Energy 2006. **80**(4): p. 383-392.
25. Zhua, M., et al., *An alternative method to predict future weather data for buildingenergy demand simulation under global climate change.* Energy and Buildings, 2016. **113**: p. 74-86.

26. Chakraborty, D., H. Elzarka, and R. Bhatnagar, *Generation of accurate weather files using a hybrid machine learning methodology for design and analysis of sustainable and resilient buildings.* Sustainable Cities and Society, 2016. **24**: p. 33-41.
27. Li, N., K. Wang, and J. Cheng, *A research on a following day load simulation method based on weather forecast parameters.* Energy Conversion and Management, 2015. **103**: p. 691–704.
28. Ignatius, M., N.H. Wong, and S.K. Jusuf, *The significance of using local predicted temperature for cooling loadsimulation in the tropics.* Energy and Buildings, 2016. **118**: p. 57-69.
29. Harlan, S.L., et al., *Neighborhood microclimates and vulnerability to heat stress* Social Science & Medicine, 2006. **63**(11): p. 2847–2863.
30. Rankin, D.W., *Mortality associated with heat wave conditions in the Melbourne metropolitan area, January and February, 1959.* Australian Meteorological Magazine, 1959. **26**: p. 96-98.
31. Smoyer-Tomic, K.E., R. Kuhn, and A. Hudson, *Heat Wave Hazards: An Overview of Heat Wave Impacts in Canada.* Natural Hazards, 2003. **28**(22): p. 465–486.
32. Coutts, A., J. Beringer, and N. Tapper, *Changing Urban Climate and CO2 Emissions: Implications for the Development of Policies for Sustainable Cities.* Urban Policy and Research 2010. **28**(1): p. 27-47.
33. Fehrenbach, U., D. Scherer, and E. Parlow, *Automated classification of planning objectives for the consideration of climate and air quality in urban and regional planning for the example of the region of Basel/Switzerland.* Atmospheric Environment, 2001. **35**: p. 5605–5615.
34. Eliasson, I., *The use of climate knowledge in urban planning.* Landscape and Urban Planning, 2000. **48**(1-2): p. 31-44.
35. Guan, L., *Preparation of future weather data to study the impact of climate change on buildings.* Building and Environment 2009. **44**: p. 793–800.
36. Guan, L., *Sensitivity of building cooling loads to future weather predictions.* Architectural Science Review, 2011. **54**(3): p. 178-191.
37. McGregor, J.L., *Regional climate modelling.* Meteorology and Atmospheric Physics, 1997. **63**(1): p. 105-117.
38. Giorgi, F. and L.O. Mearns, *Introduction to special section: Regional Climate Modeling Revisited.* Journal of Geophysical Research: Atmospheres, 1999. **104**.
39. Essenwanger, O.M., *Classification of climates*, in *World Survey of Climatology, General Climatology 1C: Classification of Climates*. 2001, Elsevier: Amsterdam. p. 102.
40. Juang, H.-M.H. and M. Kanamitsu, *The NMC Nested Regional Spectral Model.* Monthly Weather Review, 1994. **122**: p. 3-26.
41. Juang, H.-M.H., S.-Y. Hong, and M. Kanamitsu, *The NCEP regional spectral model: an update.* Bulletin of the American Meteorological Society 1997. **78**(10): p. 2125-2143.
42. Juang, H.-M.H., *The NCEP mesoscale spectral model: the revised version of the nonhydrostatic regional spectral model.* Monthly Weather Review, 2000. **128**: p. 2329-2362.
43. Chang, E.-C. and S.-Y. Hong, *Projected Climate Change Scenario over East Asia by a Regional Spectral Model.* Journal of The Korean Earth Science Society, 2011. **32**(7): p. 770-783.
44. Li, H., et al., *Projected climate change scenario over California by a regional ocean – atmosphere coupled model system.* Climatic Change, 2013. **122**(4).
45. Lee, J.-W., et al., *Future Changes in Surface Runoff over Korea Projected by a Regional Climate Model under A1B Scenario.* Advances in Meteorology, 2014. **2014**(2014).
46. Ham, S., J.-W. Lee, and K. Yoshimura, *Assessing future climate changes in the East Asian summer and winter monsoon using Regional Spectral Model.* Journal of the Meteorological Society of Japan, 2015. **94A**(2016): p. 69-87.
47. Chen, F. and J. Dudhia, *Coupling an advanced land-surface hydrology model with the Penn State/NCAR MM5 modeling system.* Monthly Weather Review, 2001. **129**(4): p. 569-585.
48. Ek, M.B., et al., *Implementation of Noah land surface model advances in the National Centers for Environmental Prediction operational mesoscale Eta model* Journal of Geophysical Research - Atmospheres, 2003. **108**(D22).

49. Hong, S.-Y. and H.-L. Pan, *Nonlocal boundary layer vertical diffusion in a medium-range forecast model.* Monthly Weather Review, 1996. **124**(10): p. 2322-2339.
50. Hong, S.-Y., H.-M.H. Juang, and Q. Zhao, *Implementation of prognostic cloud scheme for a regional spectral model* Monthly Weather Review, 1998. **126**(10): p. 2621-2639.
51. WWRP/WMO, *Recommendations for the Verification and Intercomparison of QPFs and PQPFs from Operational NWP Models*. 2008, World Meteorological Organization: Switzerland.
52. Donaldson, R.J., R.M. Dyer, and M.J. Kraus, *An Objective Evaluator of Techniques for Predicting Severe Weather Events*, in *Preprints, Ninth Conference on Severe Local Storms*, O. Norman, Editor. 1975, American Meteor Society. p. 321–326.
53. Glahn, H.R. and D.A. Lowry, *The Use of Model Output Statistics (MOS) in Objective Weather Forecasting.* Journal of Applied Meteorology, 1972. **11**(8): p. 1203-1211.
54. Klein, W.H. and H.R. Glahn, *Forecasting Local Weather by Means of Model Output Statistics.* Bulletin of the American Meteorological Society, 1974. **55**(10).
55. Ignatius, M., N.H. Wong, and S.K. Jusuf, *Urban microclimate analysis with consideration of local ambient temperature, external heat gain, urban ventilation, and outdoor thermal comfort in the tropics* Sustainable Cities and Society, 2015. **19**: p. 121-135.
56. Jusuf, S.K. and N.H. Wong, *Development of empirical models for an estate level air temperature prediction in Singapore*, in *Second International Conference on Countermeasures to Urban Heat Islands*. 2009: Berkeley, United States.
57. Jusuf, S.K., et al., *The influence of land use on the urban heat island in Singapore.* Habitat International, 2007. **31**.
58. Wong, N.H. and S.K. Jusuf, *GIS-based greenery evaluation on campus master plan.* Landscape and Urban Planning, 2008. **84**: p. 166–182.
59. Wong, N.H., et al., *Evaluation of the impact of the surrounding urban morphology on building energy consumption.* Solar Energy, 2011. **85**: p. 57-71.
60. Chong Zhun Min, A., et al., *Predicting the envelope performance of commercial office buildings in Singapore.* Energy and Buildings, 2013. **66**: p. 66-76.
61. Wong, N.H., et al., *Investigation of thermal benefits of rooftop garden in the tropical environment.* Building and Environment, 2003. **38**(2): p. 261–270.
62. Martin, M., et al., *Comparison between simplified and detailed EnergyPlus models coupled with an urban canopy model.* Submitted to Energy and Buildings, 2016.
63. NUS. *Department of Geography Weather Station*. 2016 10 August 2016]; Available from: https://inetapps.nus.edu.sg/fas/geog/.

## 9. Appendix

*Perturbation Equations of MSM*

The perturbation equations of the MSM for spectral computation related to the outer coarse base fields for three-dimensional winds, hydrostatic virtual temperature, hydrostatic surface pressure, and specific humidity are:

$$\begin{aligned} u^{*'} &= u^* - u_b^*, \\ v^{*'} &= v^* - v_b^*, \\ w' &= w - w_b, \\ \varepsilon_T \bar{T}' &= \bar{T} - T_b, \\ \varepsilon_Q \bar{Q}_s' &= \bar{Q}_s - Q_{s_b}, \\ q' &= q - q_b, \end{aligned}$$

and the perturbation virtual temperature and pressure related to the internally evolved hydrostatic virtual temperature and pressure are given as:

$$\begin{aligned} T' &= T - \bar{T} = T - \varepsilon_T \bar{T}' - T_b \; and \\ Q' &= Q - \bar{Q} = Q - \bar{Q}_s - \ln \sigma \\ &= Q - \varepsilon_Q \bar{Q}_s' - Q_{s_b} - \ln \sigma \,, \end{aligned}$$

where subscript $b$ shows variables from the coarse outer grid system and subscript $s$ shows variables on the surface. Meanwhile, $u^*$, $v^*$, and $w^*$ are wind speeds in the $x$, $y$, and $z$ directions; $T$ is virtual temperature; $q$ is specific humidity; and $Q$ is the logarithm of pressure, defined as $Q = \ln \sigma$, where $\sigma$ is the vertical coordinate, defined by $\bar{p}/\bar{p}_s$, in which $\bar{p}$ refers to hydrostatic pressure and $\bar{p}_s$ refers to hydrostatic pressure at the surface.

Here, $\varepsilon_T$ and $\varepsilon_Q$, which can be zero or one, are options for hydrostatic pressure and hydrostatic virtual temperature, respectively.

Moreover, the fully compressible non-hydrostatic system in the hydrostatic system in the hydrostatic $\sigma$ coordinate can be rewritten into a perturbation form as:

$$\begin{aligned} \frac{\partial u^{*'}}{\partial t} &= -m^2 u^* \frac{\partial u^{*'}}{\partial x} - m^2 v^* \frac{\partial u^{*'}}{\partial y} - \dot{\sigma} \frac{\partial u^*}{\partial \sigma} - E \frac{\partial m^2}{\partial x} + f v^* - R(\bar{T} + T') \frac{\partial \bar{Q}_s + Q'}{\partial x} \\ &\quad - \left(1 + \frac{T'}{\bar{T}}\right)\left(1 + \frac{\partial Q'}{\partial \ln \sigma}\right) \frac{\partial \bar{\Phi}}{\partial x} + F_{u^*} - \frac{\partial u_b^*}{\partial t}, \\ \frac{\partial v^{*'}}{\partial t} &= -m^2 u^* \frac{\partial v^{*'}}{\partial x} - m^2 v^* \frac{\partial v^{*'}}{\partial y} - \dot{\sigma} \frac{\partial v^*}{\partial \sigma} - E \frac{\partial m^2}{\partial y} - f u^* - R(\bar{T} + T') \frac{\partial \bar{Q}_s + Q'}{\partial y} \\ &\quad - \left(1 + \frac{T'}{\bar{T}}\right)\left(1 + \frac{\partial Q'}{\partial \ln \sigma}\right) \frac{\partial \bar{\Phi}}{\partial y} + F_{v^*} - \frac{\partial v_b^*}{\partial t}, \\ \frac{\partial w^{*'}}{\partial t} &= -m^2 u^* \frac{\partial v^{*'}}{\partial x} - m^2 v^* \frac{\partial w^{*'}}{\partial y} - \dot{\sigma} \frac{\partial w^*}{\partial \sigma} - g\left[1 - \left(1 + \frac{T'}{\bar{T}}\right)\left(1 + \frac{\partial Q'}{\partial \ln \sigma}\right)\right] + F_w - \frac{\partial w_b}{\partial t}, \end{aligned}$$

$$\varepsilon_Q \left\{ \frac{\partial \bar{Q}_s^{'}}{\partial t} = -m^2 \int_0^1 \left[ u^* \frac{\partial \bar{Q}_s}{\partial x} + v^* \frac{\partial \bar{Q}_s}{\partial x} + \left( \frac{\partial u^{*'}}{\partial x} + \frac{\partial v^{*'}}{\partial y} \right) \right] d\sigma - \frac{\partial Q_{s_b}}{\partial t} \right\},$$

$$\varepsilon_T \left[ \frac{\partial \bar{T}^{'}}{\partial t} = -m^2 u^* \frac{\partial \bar{T}}{\partial x} - m^2 v^* \frac{\partial \bar{T}}{\partial y} - \dot{\sigma} \sigma^K \frac{\partial \bar{T} \sigma^{-K}}{\partial \sigma} + K \bar{T} \left( \frac{\partial \bar{Q}}{\partial t} + m^2 u^* \frac{\partial \bar{Q}_s}{\partial x} + m^2 v^* \frac{\partial \bar{Q}_s}{\partial y} \right) + F_{\bar{T}} - \frac{\partial T_b}{\partial t} \right],$$

$$\frac{\partial Q^{'}}{\partial t} = -m^2 u^* \frac{\partial \bar{Q}_s + Q^{'}}{\partial x} - m^2 v^* \frac{\partial \bar{Q}_s + Q^{'}}{\partial y} - \dot{\sigma} \frac{\partial Q'}{\partial \sigma} - \frac{\dot{\sigma}}{\sigma} - \gamma \nabla_3 \cdot V^3 + \gamma \frac{F_{\bar{T}}}{T} - \frac{\partial \bar{Q}_s}{\partial t},$$

$$\frac{\partial T^{'}}{\partial t} = -m^2 u^* \frac{\partial \bar{T}_s + T^{'}}{\partial x} - m^2 v^* \frac{\partial \bar{T}_s + T^{'}}{\partial y} - \dot{\sigma} \sigma^K \frac{\partial (\bar{T} + T') \sigma^{-K}}{\partial \sigma} + K(\bar{T} + T') \left[ \frac{\partial \left( \bar{Q}_s + Q^{'} \right)}{\partial t} + m^2 u^* \frac{\partial \bar{Q}_s + Q^{'}}{\partial x} + -m^2 v^* \frac{\partial \bar{Q}_s + Q^{'}}{\partial y} + \dot{\sigma} \frac{\partial Q^{'}}{\partial \sigma} \right] + F_T - \frac{\partial \bar{T}}{\partial t}, \quad and$$

$$\frac{\partial q^{'}}{\partial t} = -m^2 u^* \frac{\partial q}{\partial x} - m^2 v^* \frac{\partial q}{\partial y} - \dot{\sigma} \frac{\partial q}{\partial \sigma} + F_{Tq} - \frac{\partial q_b}{\partial t},$$

where $t$ for temporal derivative, $g$ is the gravitational constant; $R$ is the gas constant for dry air, $m$ is a map factor, $\bar{\Phi}$ for geopotential, $V$ is vector form of horizontal wind, and $\nabla$ is two dimensional horizontal derivative on a $\sigma$ surface. $\gamma$ is defined with $C_p/C_v$, the air heat capacity for constant pressure and constant volume; hence $K = R/C_p$. Also, $\dot{\sigma}$ is vertical motion related to the $\sigma$ coordinate. Here, $F_u$, $F_v$, $F_w$, and $F_T$ are the subgrid or model physics forcings for the associated equations.